

Strangeness and Antibaryon Production in Heavy-Ion Collisions

Fuqiang Wang

Nuclear Science Division, Lawrence Berkeley National Lab, Berkeley, CA 94720

Abstract

We review the experimental results on strangeness and antibaryon production in heavy-ion collisions at the AGS and SPS. We argue that the observed enhancement in kaon production at the AGS is consistent with hadronic description, while the multistrange baryon and antibaryon results at the SPS may need physics beyond hadronic nature. We call the need for measurements of low energy antilambda-proton annihilation cross-section in the modeling of antilambda to antiproton ratio; large value of this ratio is observed in central heavy-ion collisions at the AGS and SPS. We speculate the importance of an excitation function measurement of the ratio.

1 Introduction

Nuclear matter at high energy density has been extensively studied through high energy heavy-ion collisions.¹ The primary goal of these studies is to observe the possible phase transition from hadronic matter to quark-gluon plasma (QGP),² in which quarks and gluons are deconfined over an extended region. It is believed that the QGP state existed in the early universe shortly after the Big Bang, and may still exist in the cores of today's neutron stars.³

If a QGP is created in a heavy-ion collision, the collision system will experience the states from deconfined quarks and gluons to interacting hadrons to, finally, freeze-out particles where the measurements are realized. In order to extract the information about the quark-gluon stage of heavy-ion collisions, systematic studies of multi-observables at freeze-out as a function of collision system size and bombarding energy are necessary.⁴ These observables include strangeness and antibaryon production.

Enhancement in strangeness production in high energy heavy-ion collisions over elementary nucleon-nucleon (NN) interactions has been proposed as a signature of QGP formation.^{5,6} The idea is that, in the deconfined QGP, strange quark pairs ($s\bar{s}$) can be copiously produced through gluon-gluon fusion ($gg \rightarrow s\bar{s}$),^{6,7} while in the hadronic gas, $s\bar{s}$ pairs have to be produced via pairs of strange hadrons with higher production thresholds. Moreover, the time scale of the gluon-gluon fusion process is short, on the order of 1–3 fm.⁶ On the other hand, it is argued that strangeness production rate in a chemically equilibrated hadronic gas might be as high as that in a QGP.^{7,8} However, the time needed for

a hadronic gas system to reach chemical equilibrium is significantly longer^{6,7,8} than the typical life time of a heavy-ion reaction of the order of 10 fm.

In addition to the enhanced production of strangeness, production of strange and multistrange antibaryons should be further enhanced in QGP^{8,9} under finite baryon density.^a The argument can be made in the simple Fermi energy-level picture as the following. Low energy levels of light quarks (q) are already occupied by the excessive light quarks contributing to the finite baryon density. When the Fermi energies of light quarks are higher than the bare mass of a $s\bar{s}$ pair, $s\bar{s}$ pair production is energetically more favorable than that of $q\bar{q}$. Hence, the production of nonstrange light antiquarks is suppressed, resulting in a high \bar{s}/\bar{q} ratio in QGP.

The definition of strangeness enhancement is broad. In this article, we use two types of definitions: (1) enhancement of strangeness production rate and antilambda to antiproton ($\bar{\Lambda}/\bar{p}$) ratio in central heavy-ion collisions with respect to peripheral collisions, and/or to isospin weighted NN interactions at the same energy; (2) enhancement in the ratio of strange antibaryons, $\bar{\Omega}/\bar{\Xi}$ (high strangeness content) with respect to $\bar{\Xi}/\bar{\Lambda}$ (low strangeness content).

The article is organized in the following way. In section 2, we discuss strangeness enhancement at the AGS and SPS. In section 3, we discuss strange antibaryon enhancement. Since strangeness and strange antibaryons are closely related, the discussions are necessarily coupled in these two sections. In section 4, we draw conclusions.

2 Strangeness enhancement

At AGS energy, the dominant carriers of strangeness produced in heavy-ion collisions are kaons (charged and neutral) and hyperons (Λ and Σ 's). Charged and neutral kaon yields are approximately equal under charge (isospin) symmetry. Hyperons are mostly produced through associate production with kaons. Therefore, charged kaon yields give a fairly good overall scale of strangeness production at the AGS.

Kaon yields are systematically measured by AGS E802/859/866. Fig.1 shows, in data points, kaon yields per participant as a function of the number of participants (N_p) in Si+A and Au+Au collisions.¹¹ N_p is a good indication of collision centrality under the participant-spectator picture of high energy heavy-ion collisions. The data show that kaon production rate steadily increases with collision centrality in Si+Al and Au+Au collisions. For comparison, kaon yields per participant for isospin weighted NN interactions at

^a Experimental measurements indicate that high baryon density is reached in central heavy-ion collisions at both the AGS and SPS.¹⁰

the corresponding energies are shown in Fig.1 as the open circles and squares. The enhancement factor – the ratio of kaon yields per participant in heavy-ion collisions over the same energy NN interactions – is higher in Au+Au central collisions than Si+A for both K^+ and K^- .¹¹

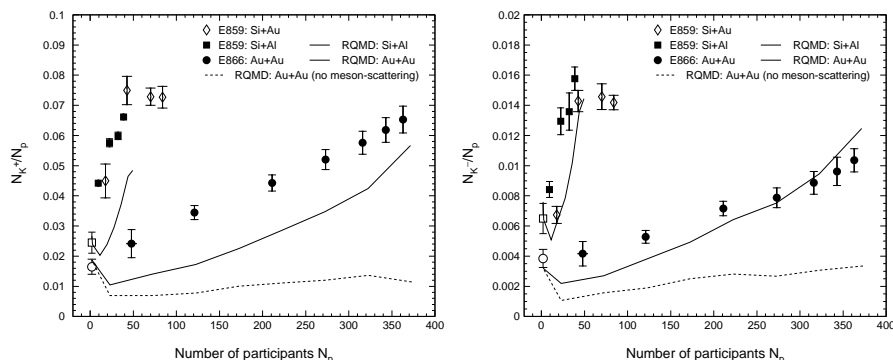


Figure 1: K^+ (left panel) and K^- (right panel) yields per participant as a function of the number of participants (N_p) for Si+A ($\sqrt{s} = 5.39$ GeV) and Au+Au ($\sqrt{s} = 4.74$ GeV) collisions at the AGS.¹¹ Those for isospin weighted NN interactions at $\sqrt{s} = 5.39$ GeV (open square) and 4.74 GeV (open dot) are also shown. RQMD results are shown in solid (the default settings) and dashed curves (meson scattering switched off). The starting point of each curve is the corresponding RQMD result for isospin weighted NN interaction. The kaon yields for both data and RQMD include ϕ feeddowns, which according to RQMD can be neglected for K^+ and increase the K^- yield by 10–15% (the default settings).

The difference between Si+A and Au+Au at the same number of participants (say $N_p \sim 50$) is qualitatively consistent with the different collision geometries under a binary collision model for kaon production, however, cannot be quantitatively explained by Glauber-type calculations of the average number of binary NN collisions.¹¹

From a classical Glauber-type picture, in which each nucleon collides multiple times with others in a heavy-ion collision, with each collision having certain probability producing kaons, one would expect higher kaon production rate in heavy-ion collisions than NN. To check this expectation, Fig.1 shows, in the dashed curves, results of RQMD calculations for Au+Au collisions with meson-baryon and meson-meson interactions switched off. One observes slight increase in kaon production rate from peripheral to central collisions. However, in contrast to the expectation, the calculated kaon production rate in heavy-ion collisions is lower than the corresponding NN value. This is probably due to the net effect of the following: (1) not all the initial nucleons collide at least

once at full energy; (2) subsequent NN collisions have less than the full energy; (3) AGS energy is near kaon production threshold where kaon production rate changes rapidly with energy in elementary p+p interactions.¹²

By including secondary meson-baryon and meson-meson interactions (the default settings), RQMD is able to describe the qualitative features seen in the data. The results of the default calculations are shown in Fig.1 as solid curves. Within the RQMD model, both baryon-baryon and meson-induced interactions increase kaon production rate. However, as seen from comparison between the dashed and solid curve (for Au+Au) in Fig.1, the meson-induced interactions dominate for kaon production, especially in central collisions.¹³ Since RQMD is a hadronic model,^b and it describes the general features of the data, it is fair to conclude that the observed kaon enhancement is consistent with hadronic physics. However, we note that subtle difference exists between the data and the default RQMD results.

As seen from Fig.1, the centrality dependences of K^+ and K^- yields are quite similar. The similarity is surprising because K^+ and K^- are thought to be produced through different mechanisms: K^- through pair production, and K^+ through both pair and associate production.

Kaon enhancement in heavy-ion collisions over NN is also observed at the SPS.¹⁴ Recent preliminary results from NA49¹⁵ show a similar centrality dependence of kaon yields as observed at the AGS.

Data on production of the more exotic multistrange baryons and antibaryons are also available at the SPS. WA97 results^{16,17} show that the Λ , Ξ and Ω midrapidity yields in the 30% most central Pb+Pb collisions are larger than those expected from p+Pb by a wounded-nucleon scaling. The effect is the largest for Ω , following the trend $\Omega > \Xi > \Lambda$. More interestingly, the Ω/Ξ ratio is larger than Ξ/Λ .¹⁷ NA49 reported results on midrapidity Ξ production in the 5% most central Pb+Pb collisions,¹⁸ consistent with the WA97 results taken into account the different centralities. Fig.2 shows the Ξ/Λ and ϕ/K ratios from NA49 (5% centrality)^{18,19}, and the Ω/Ξ ratio from WA97 (30% centrality)¹⁷ in Pb+Pb collisions. In the simple quark counting model, the particle ratios (ϕ/K^+ , Ξ^-/Λ , Ω^-/Ξ^-) present the ratio of s/q , and the antiparticle ratios (ϕ/K^- , $\Xi^-/\bar{\Lambda}$, $\Omega^-/\bar{\Xi}^-$) present the ratio of \bar{s}/\bar{q} . In Fig.2, one observes a hierarchy in the ratios: $\Omega/\Xi > \Xi/\Lambda > \phi/K$, and that the antiparticle ratios are systematically larger than the particle ratios, indicating non-vanishing baryon density at midrapidity in Pb+Pb collisions.

RQMD predictions for central Pb+Pb collisions (impact parameter $b < 4$ fm) are shown in Fig.2 as the small points connected by the lines. RQMD

^bThe non-hadronic part of RQMD, string formation and fragmentation, does not contribute significantly at AGS energy.

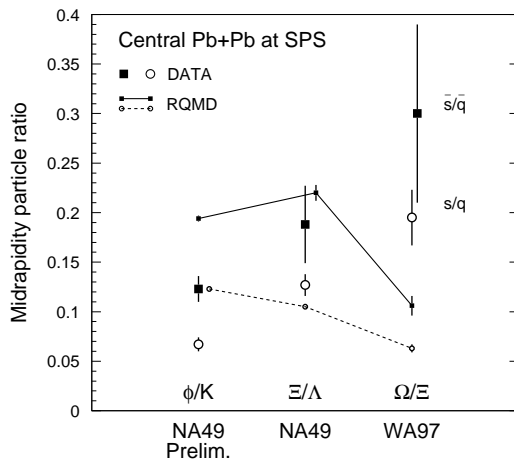


Figure 2: Midrapidity particle ratios (ϕ/K^+ , Ξ^-/Λ , Ω^-/Ξ^- in open circles) and antiparticle ratios (ϕ/K^- , $\bar{\Xi}^-/\bar{\Lambda}$, $\bar{\Omega}^-/\bar{\Xi}^-$ in filled squares) measured by NA49 (5% centrality)^{18,19} and WA97 (30% centrality)¹⁷ in Pb+Pb collisions at the SPS. The RQMD results ($b < 4$ fm) are shown in small points connected by dashed (particle ratios) and solid line (antiparticle ratios).

agrees with the Ξ/Λ data, but overpredicts ϕ/K by a factor of 1.5–2, while underpredicts Ω/Ξ by a factor of 2. The discrepancy in Ω/Ξ between the data and RQMD may due to an underestimate of the string fragmentation probability into Ω in e^+e^- , used in RQMD.²⁰ An even larger discrepancy is seen between data and URQMD model prediction.²¹ Presumably, the better agreement between data and RQMD than URQMD is due to the novel “rope” mechanism,²² implemented in RQMD but not in URQMD. However, the “rope” mechanism is clearly beyond the scope of hadronic physics.

3 Antibaryon enhancement

As discussed in the introduction, enhancement in strange antibaryon production is a possible signature for QGP formation. Preliminary results from AGS E859 indicate a large $\bar{\Lambda}/\bar{p}$ ratio in Si+Au central collisions near midrapidity.²³ Direct measurement of $\bar{\Lambda}$ production in Au+Au collisions at the AGS was not available until recently.²⁴ However, the $\bar{\Lambda}/\bar{p}$ ratio can be inferred from \bar{p} measurements in the midrapidity region by E864^{25,26} and E878²⁷ at $p_T \approx 0$ with different acceptances for \bar{p} from weak decays ($\bar{\Lambda} + \bar{\Sigma}^0$ and $\bar{\Sigma}^+$), provided

that the experimental acceptances and systematics are well understood. The obtained $(\overline{\Lambda} + \overline{\Sigma}^0 + 1.1\overline{\Sigma}^+)/\overline{p}$ ratio increases strongly with collision centrality, with a most probable value of 3.5 in the 10% most central collisions.²⁶

Assuming $\overline{\Sigma}$ yield of each sign is 1/3 of $\overline{\Lambda}$ yield under isospin consideration,^c the $\overline{\Lambda}/\overline{p}$ ratio can be deduced. Further using the E866 measurements of \overline{p} 's which include 60% weak decay \overline{p} 's,²⁸ the yields of \overline{p} and $\overline{\Lambda}$ can be obtained, the results of which are shown in Fig.3 against collision centrality. The recent direct measurements of \overline{p} and $\overline{\Lambda}$ yields by E917²⁴ are plotted as filled points. They agree with the obtained systematics, although suffering from large statistical errors.

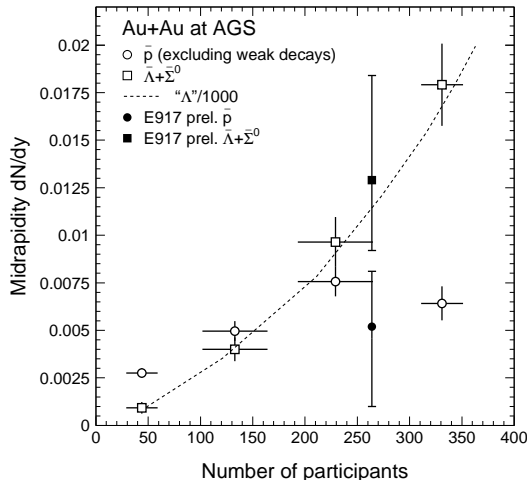


Figure 3: Midrapidity yields of $\overline{\Lambda} + \overline{\Sigma}^0$ and \overline{p} (excluding weak decay products) as a function of collision centrality in Au+Au collisions at the AGS, deduced from midrapidity \overline{p} measurements by E866²⁸ and the most probable $(\overline{\Lambda} + \overline{\Sigma}^0 + 1.1\overline{\Sigma}^+)/\overline{p}$ ratio by E864²⁶, assuming $\overline{\Sigma}^0 = \overline{\Sigma}^+ = \frac{1}{3}\overline{\Lambda}$ under isospin consideration. “ Λ^* ”= $K^+ - K^-$ by the constrain of overall strangeness neutrality and the assumption of $K^+ - K^- = K^0 - \overline{K}^0$ and $\Lambda = \Sigma$.

As seen from Fig.3, \overline{p} yield increases from peripheral to medium central collisions, and saturates (or even slightly decreases) in central collisions. This is consistent with the picture that more \overline{p} 's are absorbed in the nuclear medium in central collisions with higher baryon density and/or larger collision zone.

^c The assumption does not account for the mass difference between $\overline{\Lambda}$ and $\overline{\Sigma}$, which may yield a deviation from 1/3 in a thermal model argument. However, the assumption of 1/3 is fairly consistent with RQMD and VENUS model calculations.

However, the continuous increase of the $\bar{\Lambda}$ yield is surprising. In the additive quark model, $\bar{\Lambda}N$ annihilation cross section is $2/3$ of $\bar{p}N$'s, therefore, a strong absorption of $\bar{\Lambda}$ should also occur.

Because of the lack of $\bar{\Lambda}N$ annihilation cross-section data at the relevant low energy (~ 1 GeV), hadronic models have to make assumptions for the cross-section to calculate $\bar{\Lambda}/\bar{p}$. Cascade calculations by Wang *et al.*,²⁹ using various parameterizations for the $\bar{\Lambda}N$ annihilation cross-section, fail to describe the observed $\bar{\Lambda}/\bar{p}$ in central collisions, while giving reasonable agreement to the peripheral collision data.

It would be interesting to compare the centrality dependences of $\bar{\Lambda}$ and Λ yields. Since the Λ yield centrality dependence at the AGS is presently not available, we use the difference in K^+ and K^- yields to reflect the Λ yield, exploiting the constrain of overall strangeness neutrality, and further assuming $K^+ - K^- = K^0 - \bar{K}^0$ and $\Lambda = \Sigma$ under isospin consideration. The results are shown in Fig.3 as the dashed curve. It is interesting to note that the centrality dependences of the Λ and $\bar{\Lambda}$ yields are very similar, a feature also observed for K^+ and K^- yields.

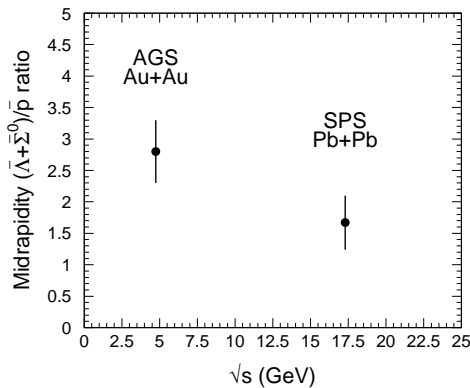


Figure 4: Midrapidity $(\bar{\Lambda} + \bar{\Sigma}^0)/\bar{p}$ ratios in central collisions of Au+Au at the AGS and Pb+Pb at the SPS.

From the centrality dependence of $\bar{\Lambda}/\bar{p}$, it is hard to disentangle the two different effects, QGP formation and strong medium absorption, both giving an increasing $\bar{\Lambda}/\bar{p}$ with centrality. It is therefore attempting to examine the ratio as a function of collision energy, which is shown in Fig.4.^d The two effects

^d The ratio for Pb+Pb at the SPS is derived from several measurements.^{17,30}

would give different dependences: at high energy, QGP formation would result in a high ratio, while strong absorption would result in a low ratio because the baryon density is lower at high energy.^{10,31} Therefore, an increase of $\bar{\Lambda}/\bar{p}$ with collision energy would indicate QGP formation or other new physics. From the current data shown in Fig.4, we cannot draw conclusions. Data at other energies are therefore highly desirable.

The $\bar{\Omega}/\bar{\Xi}$ and $\bar{\Xi}/\bar{\Lambda}$ ratios discussed in section 2 are significantly lower than $\bar{\Lambda}/\bar{p}$ shown in Fig.4 for Pb+Pb central collisions. This points to the speculation that medium absorption of strange antibaryons may be very different from that of antiprotons. Again, measurements of low energy $\bar{\Lambda}N$ annihilation cross-sections are indispensable.

4 Conclusions

We reviewed the AGS and SPS data on strangeness and antibaryon production. We draw the following conclusions:

- Enhancement in charged kaon production is observed in central heavy-ion collisions at the AGS with respect to peripheral collisions and isospin weighted nucleon-nucleon interactions. The enhancement can be qualitatively explained by secondary particle scattering within the RQMD model. However, subtle difference exists between the data and RQMD.
- A hierarchy of particle ratios, $\Omega/\Xi > \Xi/\Lambda > \phi/K$, is observed at midrapidity in Pb+Pb central collisions at the SPS. The antiparticle ratios are systematically larger than the particle ratios. RQMD with string and rope formation and fragmentation, which is clearly beyond hadronic physics, may barely describe the data.
- Large $\bar{\Lambda}/\bar{p}$ ratios are observed in central heavy-ion collisions at the AGS and SPS. Strong increase of the ratio from peripheral to central collisions is indirectly observed at the AGS. Hadronic cascade calculations, with certain assumptions for the $\bar{\Lambda}N$ annihilation cross-section, fail to describe the ratio in central collisions.
- To fully understand the $\bar{\Lambda}/\bar{p}$ ratio in heavy-ion collisions, measurements of low energy $\bar{\Lambda}N$ annihilation cross-sections are needed. On the other hand, an excitation function measurement of $\bar{\Lambda}/\bar{p}$ may provide a new avenue in the search for QGP.

Acknowledgments

I am especially grateful to Professor R.K. Seto for inviting me to review the experimental results. I would like to thank Drs. A.M. Poskanzer, H.G. Ritter, N. Xu, and other members of the LBNL/RNC group for fruitful discussions. This work was supported by the U.S. Department of Energy under contract DE-AC03-76SF00098.

References

1. For recent developments, see Quark Matter '96 proceedings, *Nucl. Phys.*, A610, 1996; and Quark Matter '97 proceedings, *Nucl. Phys.*, A638, 1998.
2. T.D. Lee and G.C. Wick, *Phys. Rev. D*, 9:2291, 1974; T.D. Lee, *Rev. Mod. Phys.*, 47:267, 1975; B.A. Breedman and L.D. McLerran, *Phys. Rev. D.*, 16:1169, 1977; E.V. Shuryak, *Phys. Lett.*, 81B:65, 1979; L. McLerran, *Rev. Mod. Phys.*, 58:1021, 1986.
3. B.D. Keister and L.S. Kisslinger, *Phys. Lett. B*, 64:117, 1976; N.K. Glendenning, S. Pei, and F. Weber, *Phys. Rev. Lett.*, 79:1603, 1997.
4. S.A. Bass *et al.*, *J. Phys. G*, 25:R1, 1999.
5. J. Rafelski and B. Müller, *Phys. Rev. Lett.*, 48:1066, 1982; J. Rafelski, *Phys. Rep.*, 88:331, 1982; R. Koch, B. Müller, and J. Rafelski, *Phys. Rep.*, 142:167, 1986.
6. H. C. Eggers and J. Rafelski, *Int. J. Mod. Phys.*, A6:1067, 1991.
7. J. Kapusta and A. Mekjian, *Phys. Rev. C*, 33:1304, 1986.
8. K.S. Lee, M.J. Rhoades-Brown, and U. Heinz, *Phys. Rev. C*, 37:1452, 1988.
9. C. M. Ko, M. Asakawa, and P. Levai, *Phys. Rev. C*, 46:1072, 1992.
10. L. Ahle *et al.* (E802 Coll.), *Phys. Rev. C*, 57:R466, 1998; H. Appelshäuser *et al.* (NA49 Coll.), *Phys. Rev. Lett.*, 82:2471, 1999.
11. L. Ahle *et al.* (E802 Coll.), nucl-ex/9905001, 1999.
12. E. Albin *et al.*, *Nucl. Phys.*, B84:269, 1975.
13. H. Sorge *et al.*, *Phys. Lett. B*, 271:37, 1991.
14. J. Bartke *et al.* (NA35 Coll.), *Z. Phys. C*, 48:191, 1990; T. Alber *et al.* (NA35 Coll.), *Z. Phys. C*, 64:195, 1994; C. Bormann *et al.* (NA49 Coll.), *J. Phys.*, G23:1817, 1997; H. Bøggild *et al.* (NA44 Coll.), *Phys. Rev. C*, 59:328, 1999.
15. F. Sikler (NA49 Coll.), Quark Matter '99 proceedings.
16. E. Andersen *et al.* (WA97 Coll.), *Phys. Lett. B*, 433:209, 1998.
17. I. Kralik *et al.* (WA97 Coll.), *Nucl. Phys.*, A638:115c, 1998.
18. H. Appelshäuser *et al.* (NA49 Coll.), *Phys. Lett. B*, 444:523, 1998.
19. F. Pühlhofer (NA49 Coll.), *Nucl. Phys.*, A638:431c, 1998; G. Roland

- (NA49 Coll.), *Nucl. Phys.*, A638:91c, 1998.
20. H. Sorge, private communication.
 21. S.A. Bass, private communication.
 22. H. Sorge *et al.*, *Phys. Lett. B*, 289:6, 1992; H. Sorge, *Phys. Rev. C*, 52:3291, 1995.
 23. Y. Wu (E802 Coll.), Wayne State University report WSU-NP-96-16, 37, 1996; G.S.F. Stephans and Y. Wu (E802 Coll.), *J. Phys. G*, 23:1895, 1997.
 24. W. Chang *et al.* (E917 Coll.), nucl-ex/9904010, 1999; G. Heintzelman (E917 Coll.), this proceedings.
 25. T.A. Armstrong *et al.* (E864 Coll.), *Phys. Rev. Lett.*, 79:3351, 1997.
 26. T.A. Armstrong *et al.* (E864 Coll.), *Phys. Rev. C*, 59:2699, 1999.
 27. D. Beavis *et al.* (E878 Coll.), *Phys. Rev. Lett.*, 75:3633, 1995; M.J. Bennett *et al.* (E878 Coll.), *Phys. Rev. C*, 56:1521, 1997.
 28. L. Ahle *et al.* (E802 Coll.), *Phys. Rev. Lett.*, 81:2650, 1998.
 29. G.J. Wang *et al.*, nucl-th/9807036, 1998.
 30. R. Lietava *et al.* (WA97 Coll.), *J. Phys. G* 25:181, 1998; M. Kaneta *et al.* (NA44 Coll.), *Nucl. Phys.*, A638:419c, 1998.
 31. F. Wang (NA49 Coll.), nucl-ex/9812001, 1998.